nature immunology

Self-reactivity in thymic double-positive cells commits cells to a CD8αα lineage with characteristics of innate immune cells

Tetsuya Yamagata, Diane Mathis & Christophe Benoist

Thymocytes displaying self-reactive T cell receptors usually undergo negative selection in the thymus. Here we demonstrate that agonist peptides can promote positive selection of immature double-positive thymocytes into distinct lineages, varying with the agonist concentration and the animal's age. Microarray gene expression analyses showed broad transcriptional alterations in a set of transcripts associated with the innate immune system, as well as silencing of CD8β expression. The resulting CD8αα T cells showed a rapid effector cytokine response. Hence, T cells displaying self-reactive receptors can have the gene expression profile and phenotypic characteristics of innate immune cells.

The constellation of self peptides that differentiating T lymphocytes encounter in the thymus is essential in shaping the preimmune repertoire. The consensus, based mainly on results from studies of TCR-transgenic systems, is that immature thymocytes that interact strongly with cognate self peptide in the context of appropriate major histocompatibility complex (MHC) molecules (agonist) are negatively selected, resulting in deletion of self-reactive clones. Those thymocytes whose TCRs bind to MHC molecule–self peptide complexes with moderate affinities are positively selected for further maturation, and quantitative differences in the strength of the positively selecting signal may condition the choice of lineage toward the $CD4^+$ or $CD8^+$ compartment[1].

There have been exceptions to this view, however, in reports of involvement of agonist peptides in thymocyte positive selection. Early studies using fetal thymic organ culture (FTOC) showed that low doses of agonist peptide promoted positive selection of CD8 single-positive (SP) T cells in MHC class I–restricted TCR-transgenic systems[2,3], although the functional relevance of the cells thus elicited was later questioned[4–6]. Later experiments produced analogous results in an MHC class II–restricted TCR-transgenic system[7], and there have been similar findings *in vivo* with animals that expressed TCRs recognizing neoantigens[8]. In addition, correlations have been made between thymocyte recognition of agonist ligands in the thymus and the adoption of a regulatory phenotype ($CD4^+CD25^+$ 'regulatory' T cells or natural killer (NK) T cells)[9–11].

Despite such reports, positive selection by agonist peptide remains intrinsically difficult to comprehend. Why would the immune system accept the danger of maintaining potentially harmful self-reactivity? The dogma has been that thymocytes capable of reacting strongly to MHC–self peptide complexes must be eliminated or silenced in the thymus to avoid autoimmune pathology in the periphery. Indeed, the purging of self-reactive T cells through strong TCR engagement is a basic tenet of central tolerance[12–14], and recent findings with mice defective in thymic expression of 'peripheral' organ-specific antigens have re-emphasized the importance of central tolerance in avoiding organ-specific autoimmune diseases[15].

Here we undertook a series of experiments to explore the influence of agonists on differentiation programs. We found that strong agonist ligands of TCRs could promote thymocyte maturation along divergent pathways of differentiation to cells of conventional or innate-like characteristics as a function of agonist dose.

RESULTS

Agonist positively selects HY TCR–bearing CD8 SP cells

We initially designed experiments to investigate the early events that unfold after immature $CD4^+CD8^+$ double-positive (DP) thymocytes encounter selecting MHC molecules on the surfaces of thymic stromal cells (TSCs). We used a reaggregation thymic organ culture (RTOC) system[16] whose input was preselected DP cells derived from TCR-transgenic mice mixed with TSCs from deoxyguanosine-treated embryonic thymi. To achieve monoclonality, we bred mice with the TCR transgenes onto a recombination activating gene (RAG)–deficient background, and to ensure their 'ignorance' of selection signals, we propagated the HY TCR–transgenic line ($H\text{-}2^b$-restricted and reactive to a male-specific peptide of Smcy) on a nonselecting $H\text{-}2^{d/d}$ background. In this genetic context, neither positive nor negative selection of HY TCR–transgenic thymocytes occurs, as their maturation is completely blocked at the DP stage[17]. Positive selection into the CD8 SP compartment can be synchronously initiated by the addition of TSCs

Section on Immunology and Immunogenetics, Joslin Diabetes Center; Department of Medicine, Brigham and Women's Hospital; Harvard Medical School; One Joslin Place, Boston, Massachusetts 02215, USA. Correspondence should be addressed to D.M. or C.B. (cbdm@joslin.harvard.edu).

Published online 9 May 2004; doi:10.1038/ni1070

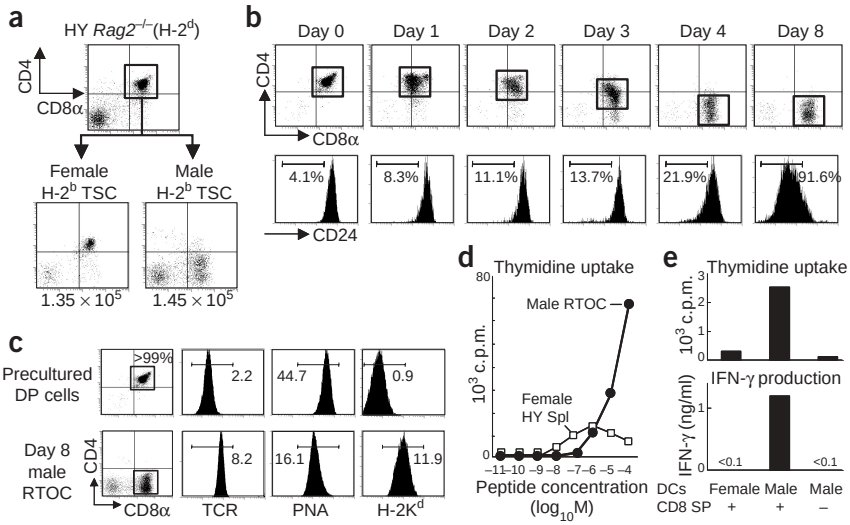

Figure 1 Agonist peptide restores positive selection in defective thymi from HY TCR–transgenic female mice. (**a**) RTOC of unselected DP cells (boxed) from HY *Rag2*$^{-/-}$ H-2^{d} thymi mixed with 'gender-sorted' fetal TSCs (cultured in deoxyguanosine). Reaggregated lobes were cultured for 4 d and were analyzed by flow cytometry; profiles are representative of more than eight independent experiments. (**b**) RTOC of HY RAG2-deficient DP cells and TSCs from male mice, stained for CD4 versus CD8, or CD24 (gated on boxed population; data represent percent CD24^{lo} cells). Time, above dot plots. Numbers in histograms indicate percentage of cells within bracketed section. (**c**) Sorted DP cells from young HY RAG2-deficient mice were cultured by RTOC with TSCs from male mice, and stained before or after (each boxed) culture with antibodies to TCR (V$_{\beta}$8) or H2-K^{d}, or with peanut agglutinin (PNA). Number in dot plot indicates the percentage of cells in that quadrant; numbers in histograms indicate mean fluorescence intensity (MFI) of cells within bracketed section. (**d**) CD8 SP cells from male RTOC (day 8) were sorted and stimulated with Smcy peptide presented by B6 splenocytes, and proliferation was measured as thymidine incorporation at 48 h. Female HY spl, splenocytes from female HY mice. (**e**) As described in **d**, but with purified male or female DCs as stimulators; stimulation was measured as proliferation or release of IFN-γ into the supernatant (enzyme-linked immunosorbent assay).

that present appropriate MHC-peptide complexes. When highly purified DP thymocytes from H-2$^{d/d}$ HY TCR–transgenic RAG2-deficient mice were reaggregated with TSCs from H-2$^{b/b}$ mice, the TSCs from female mice elicited very little positive selection; in contrast, TSCs from male mice selected a robust cohort of CD8 SP cells (**Fig. 1a**). Total cell yields were equivalent in both cultures. The selection of CD8 SP cells by TSCs from male mice was not due to coreceptor crosslinking by the antibodies used for cell sorting, as such cells were also generated from unsorted thymocytes (data not shown). Selection by TSCs from male mice did not depend on the presence or absence of residual CD45^{+} antigen-presenting cells (APCs; data not shown). In contrast to published data[18], pre-exposure to APCs 'loaded' with agonist ligand did not influence the outcome (data not shown).

A time course analysis showed that the CD8 SP cells were generated from DP cells, with a gradual and mostly synchronous shift of the CD4 and CD8 staining patterns and a progressive reduction of the CD24 'immaturity marker' (**Fig. 1b**). This ruled out the possibility that the CD8 SP cells originated from expansion of a minor pre-existing contaminant population, a conclusion confirmed by fluorescence labeling of input DP cells: less than half of the cells had cycled by day 4, and most of them did so for one cycle only (data not shown). Thus, HY TCR–transgenic DP thymocytes that are blocked in differentiation can be positively selected by high-affinity agonist.

Further analysis of cell surface markers confirmed the mature phenotype of the CD8 SP cells selected by RTOC with agonist ligand: upregulation of TCR and H2-K^{d} molecules and loss of peanut agglutinin–binding glycosylation occurred (**Fig. 1c**). Published results have indicated that thymocytes selected by agonist peptide in full FTOC were anergized[4–6]. Here, purified CD8 SP cells retained the ability to respond to APCs loaded with Smcy peptide, with a higher optimum peptide concentration than HY splenocytes from female mice (**Fig. 1d**). Similarly, and in response to a more physiological ligand, CD8 SP cells proliferated and produced interferon-γ (IFN-γ) when confronted with agonistic dendritic cells (DCs) from male, but not female, mice (**Fig. 1e**). These data show that CD8 SP cells selected by agonist ligand presented on RTOC epithelial cells are phenotypically mature and antigen responsive.

Different agonist concentrations select different phenotypes

We tested the sensitivity of the positive selection process induced by agonist by supplementing TSCs from female mice with graded doses of the agonist Smcy peptide (**Fig. 2a**). The selection of TCR^{hi} CD8 SP cells was very efficient at 10 nM peptide, which compares favorably with the optimum 1 μM concentration for stimulation of mature HY splenocytes (**Fig. 1d**). From 10 nM to 1 μM peptide, the selected cells showed a 'tight' profile of CD8 expression, but above 1 μM their density of surface CD8 was reduced and became more heterogeneous. Only at 100 μM did negative selection set in. Costaining with antibody to CD8α (anti-CD8α) and anti-CD8β showed that with 100 nM peptide, almost all selected CD8 SP cells expressed the CD8αβ heterodimer; higher peptide concentrations resulted in the loss of CD8β, leaving the cells expressing exclusively the CD8αα homodimer. Thus, low-dose agonist selects CD8αβ cells, whereas a higher dose selects CD8αα cells. The last results are reminiscent of the enhanced selection of CD8αα intraepithelial lymphocytes (IELs) in the H-Y male mice[19–21] and of agonist-supplemented FTOC[22–24].

Positive selection by agonist ligand *in vivo*

The inability of TSCs from female mice and potent ability of TSCs from male mice to promote positive selection of DP thymocytes from HY TCR–transgenic mice seems at odds with the common perception of these mice as the archetype of clonal deletion. There is, however, some precedent for poor positive selection in young female mice[25] and 'escape' of clonotype-positive cells in male mice[26]. Thus, we re-examined the thymi of HY TCR–transgenic mice (H-2^{b}-selecting background) of different ages. The adult female thymus contained many CD8 SP cells, but these were mostly absent in the first weeks of age (**Fig. 2b**, top), consistent with published results[25]. In contrast, the male HY thymus contained greater numbers of mature cells at early ages (**Fig. 2b**, bottom, 1–2 weeks). As in the RTOC, many of these cells lacked CD8β and displayed the CD8αα homodimer. With age, the thymi of HY males showed a persistence of some mature CD8 SP cells but an increase in double-negative cells[27]. Thus, positive selection of mature CD8 SP cells by male antigen and loss of CD8β both occur preferentially in young mice, as also found in the RTOC system.

MHC class–independent selection of CD8αα cells

We next sought to determine whether the agonist-induced selection of DP cells into the CD8αβ and CD8αα SP compartments was a 'quirk' of HY thymocytes. We reaggregated DP cells expressing two other TCRs on a nonselecting background (RAG-deficient mice also deficient in transporter associated with antigen processing, with a nonselecting MHC) with TSCs displaying the appropriate MHC molecules, and supplemented cultures with various doses of the relevant agonist peptides. The OT-1 TCR recognizes an ovalbumin peptide presented by H-2K^b molecules, and thymocytes expressing this receptor are positively selected to become CD8αβ SP cells when reaggregated with H-2^b TSCs. With the addition of 10 pM ovalbumin peptide to the culture, CD8 SP cells retained CD8β expression, but at a higher concentration (100 pM) the cells became CD8αα (**Fig. 3a**). We noted a similar phenotypic switching with the MHC class II–restricted 5CC7 TCR that recognizes moth cytochrome *c* peptide in the context of H-2E^k (ref. 28); its selection requires H-2E^k and the set of peptides normally loaded in the presence of the invariant chain. When nonselected (H-2^b) 5CC7 DP thymocytes were reaggregated with TSCs prepared from H-2^k invariant chain–null mice, the cells remained mostly double positive in the culture because of limited peptide presentation on invariant chain–deficient TSCs (**Fig. 3b**, left). The addition of 1 nM moth cytochrome *c* peptide agonist peptide induced selection into both the CD8αβ SP and CD4 SP compartments (**Fig. 3b**, middle). At a higher dose, however, CD4 SP cells disappeared, and the only CD8 SP cells that remained had extinguished CD8β expression. (**Fig. 3b**, right). Thus, in three different TCR transgenic systems, CD8αβ SP cells are produced at low doses of agonist peptide, and CD8αα cells are produced at higher doses. We found less clonal deletion here than was found in earlier studies using FTOCs[3,4,29] that were subject to negative selection at the DN or DN→DP stages.

Microarrays show broadly distinct differentiation programs

The data presented above indicate that positive selection can occur when TCR-transgenic thymocytes encounter agonist MHC-peptide ligand in the thymus, producing cells of two apparently different phenotypes depending on peptide concentration. These findings raise two important questions. Although they seem phenotypically normal (**Figs. 1** and **2**), are the CD8αβ SP cells that are selected by agonist MHC-peptide different from those normally selected on MHC-self peptide ligands? And is the CD8β chain downregulation found at higher agonist doses isolated or does it denote a true lineage shift? To address these, we did a microarray analysis of cell populations elicited by the three distinct conditions (natural ligands, low-concentration agonist and high-concentration agonist).

We prepared RNA from the CD8αβ and CD8αα cells that emerged from HY DP cells after the addition of low- and high-dose agonist (100 nM and 10 μM Smcy, respectively; **Fig. 2a**). CD8αβ cells generated from OT-1 DP cells in RTOC without peptide addition represented cells selected by natural ligands (**Fig. 3a**, left). In all cases, we sorted input DP thymocytes from mice carried on the nonselecting background, permitting a 'clean' analysis of events occurring after TCR engagement by ligands displayed on the surfaces of TSCs. We sorted positively selected CD8 SP cells from four independent RTOCs at day 6 of culture.

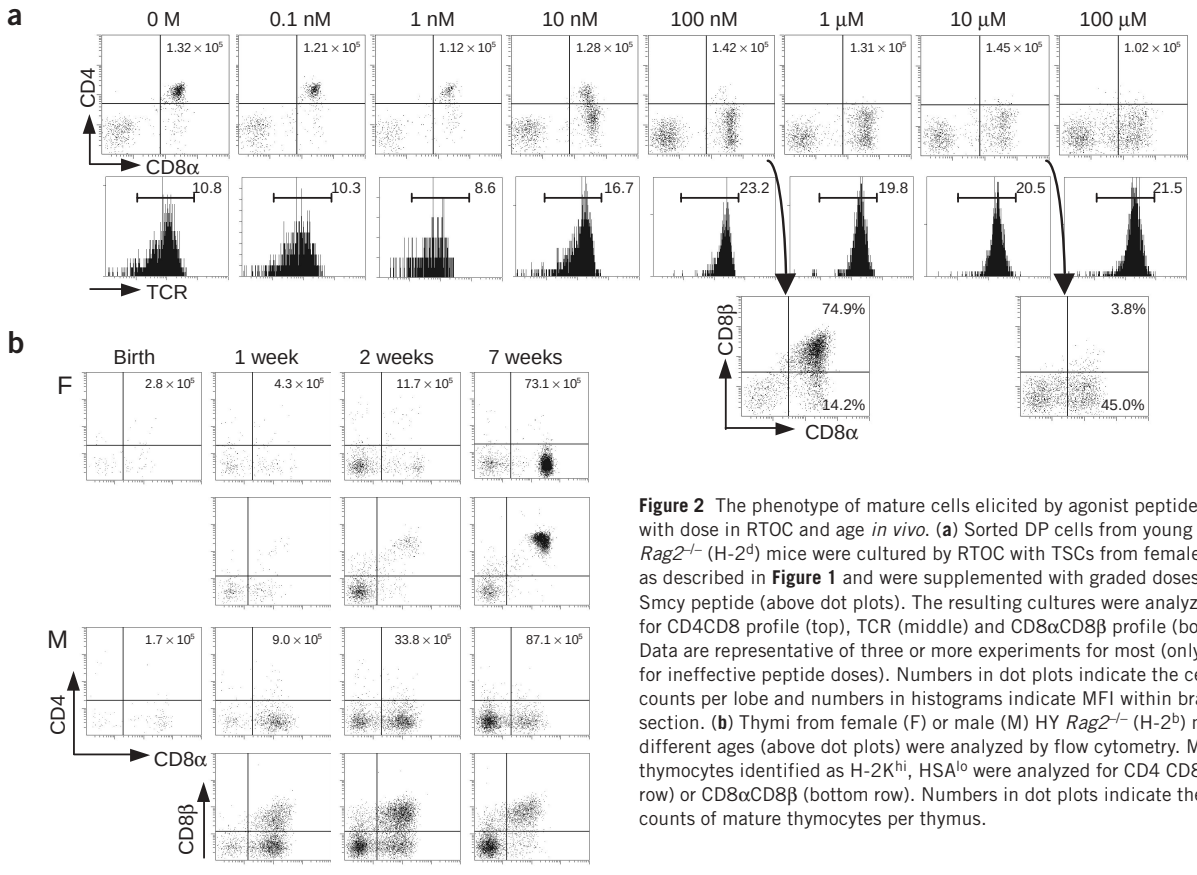

Figure 2 The phenotype of mature cells elicited by agonist peptide varies with dose in RTOC and age *in vivo*. (**a**) Sorted DP cells from young HY *Rag2*$^{-/-}$ (H-2^d) mice were cultured by RTOC with TSCs from female mice as described in **Figure 1** and were supplemented with graded doses of Smcy peptide (above dot plots). The resulting cultures were analyzed for CD4CD8 profile (top), TCR (middle) and CD8αCD8β profile (bottom). Data are representative of three or more experiments for most (only two for ineffective peptide doses). Numbers in dot plots indicate the cell counts per lobe and numbers in histograms indicate MFI within bracketed section. (**b**) Thymi from female (F) or male (M) HY *Rag2*$^{-/-}$ (H-2^b) mice of different ages (above dot plots) were analyzed by flow cytometry. Mature thymocytes identified as H-2K^{hi}, HSA^{lo} were analyzed for CD4 CD8α (top row) or CD8αCD8β (bottom row). Numbers in dot plots indicate the cell counts of mature thymocytes per thymus.

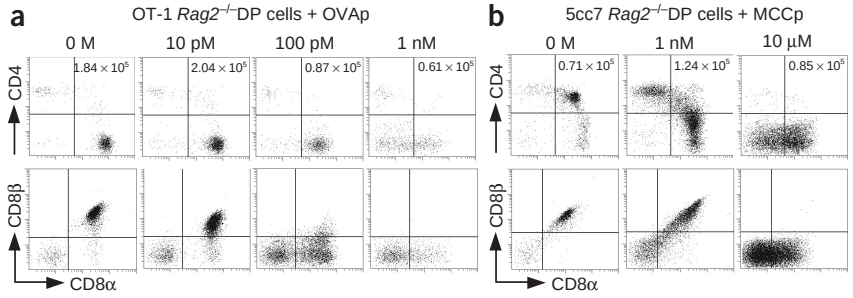

Figure 3 Mature CD8αα cells of other TCR specificities are elicited by their cognate peptide. Unselected DP cells from two different TCR-transgenic mice, MHC class I–restricted OT-1 (**a**) and MHC class II–restricted 5CC7 (**b**), were cultured by RTOC with graded doses (above dot plots) of the relevant agonist peptide (ovalbumin peptide (OVAp) or moth cytochrome *c* peptide (MCCp), respectively). The cultures were stained for CD4 CD8 or CD8α CD8β after 4 d in culture. Results are representative of three or more experiments. Numbers in dot plots indicate cell counts per lobe.

We did four independent hybridizations to Affymetrix Mu74Av2 chips. All raw data sets have been deposited, and processed values and complete gene lists and tables are available (**Supplementary Table 1** online). Raw hybridization data were processed with the MAS (Affymetrix) or RMA[30] algorithm and normalized, and composite expression values were calculated for each of the 12,488 genes on the chip (averaging after outlier elimination; DISTILL software). We did many bioinformatic analyses of the data sets. Here we call CD8 cells selected on natural ligands 'O cells', agonist-selected CD8αβ cells 'AB cells', and agonist-selected CD8αα cells 'AA cells'.

The data obtained substantiate the validity and accuracy of the analysis (**Fig. 4a**). We plotted relative expression differences for all 12,488 genes on the microarray, comparing the AA and AB populations relative to O as a common frame of reference (plotting AA/O versus AB/O 'fold changes'). Many of the genes that appeared as differentially transcribed represent internal controls (**Fig. 4a**, green dots). For example, HY and OT-1 TCR–transgenic thymocytes were consistently obtained from female and male donors, respectively, and this was reflected by high AA/O and AB/O ratios for *Xist* (X-inactivating transcript) and low AA/O and AB/O ratios for *Ddx3y* (previously known as *Dby*) and *Eif2s3y* (Y chromosome genes). Values for MHC molecules or TCR variable (V) regions also matched the patterns expected from the cells' genotypes. These 'controls' were excluded from all subsequent analyses. Also conforming to prediction was *Cd8b*, not expressed by the AA population (**Fig. 4a**, red dot).

For an overall assessment of the relationships between the differently selected populations, we estimated the overall distance between them as an aggregate of expression differences across many genes (Euclidian distance; **Fig. 4b**); we calculated the distances for genes that showed 'fold changes' greater than 3 or 6 in any one comparison, to avoid confounding 'noise' generated by the large number of genes that show background variation only. We compared the values obtained with those derived by parallel calculations done on mock data sets generated by random permutation between sample types obtained to model the experimental noise inherent to the multiple sampling of microarray experiments. Based on the distances calculated in this way, we drew triangles showing the relationships between the three populations (**Fig. 4b**). Two points can be made from this representation of the data: the distance between the O and AB populations was not significantly greater than that found with randomized data ($P = 0.17$), and the AA population was significantly different from the other two ($P < 10^{-6}$). The triangles 'leaned' to the right, suggesting that AA was slightly closer to AB than to O. These distances reflected the input from a large number of genes and, although it showed the most notable change in expression, *Cd8b* made only a minor contribution to the overall distance (data not shown). These distance metrics suggest that the CD8αβ SP cells elicited by agonist ligands were not substantially different from natural CD8 SP cells, as the agonist peptide and self peptide signals induced very similar profiles of global gene expression; and that CD8αα cells stem from an altered gene expression program, one much more profound than the simple downregulation of CD8β.

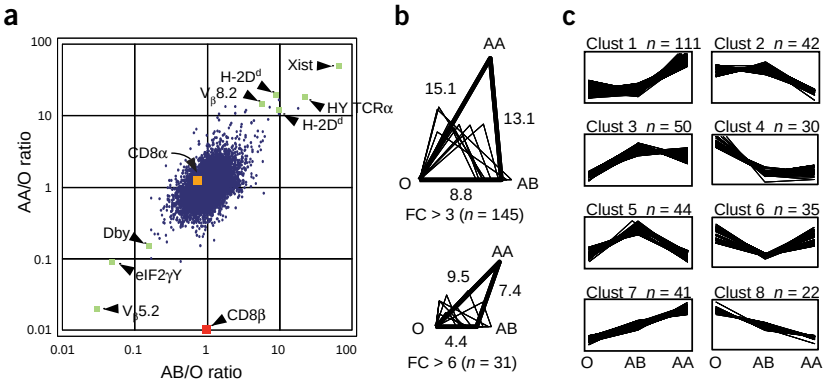

Figure 4 CD8αα cells have a distinct gene expression profile. (**a**) Validation of the microarray analysis. Agonist-selected CD8αα (AA), CD8αβ (AB) or naturally selected CD8αβ (O) populations were purified by cell sorting, and the resulting RNA was used to probe Affymetrix Mu74Av2 chips. Expression values were calculated as the average in four independent experiments, with outlier elimination. Data compare the AA/O and AB/O ratios of expression values; each dot represents an independent feature (gene) of the chip. Green dots, 'control' genes (specific for gender, TCR or MHC allele) whose expression was expected to be different, given the origin of the cells; orange and red dots, CD8α and CD8β genes, respectively, whose variations were also expected on the basis of cell surface phenotypes. (**b**) Analysis of 'distance' between populations. Euclidian distance between AA, AB and O populations, calculated from 'means-normalized' expression values, restricted to genes having an expression value of 10 (range, 1–5,000) to limit noise (which is very high in low expression ranges after processing with MAS 5.0 software) and a 'fold change' (FC) of at least 3 or 6 (top and bottom, respectively) in any one comparison. Thin lines represent the random data sets. (**c**) Cluster analysis of gene expression. The 'cor' function in S-Plus was used to group genes that show correlated expression profiles in the O, AA and AB populations (vertical axis, relative expression value, calculated as the expression value in each population divided by the 'gene-wise' means). Clust, cluster.

We then applied correlation analysis to identify the actual genes underlying these global distances. To reduce background noise, we focused the analysis on a set of 375 'informative' genes (that is, filtered on expression levels greater than 3 in any one population and on showing a 'fold change' greater than 3 in any one comparison). This analysis yielded eight dominant clusters (**Fig. 4c**). The main cluster represented 111 genes more highly expressed in AA than in AB or O (**Fig. 4c**, Clust 1). With its 'mirror image' (**Fig. 4c**, Clust 2), it accounted for 40.6% of the informative genes (153 of 375), consistent with the distance calculations (**Fig. 4b**). Other clusters were smaller and were not dissimilar in number to 'pseudo-clusters' obtained with the randomized data sets (data not shown).

We also obtained a more detailed view of those genes specifically overexpressed in AA (**Fig. 5a**, highlighted). There was a high occurrence of genes normally associated with innate immune system cells, in particular NK cells (**Fig. 5a**). These include genes encoding cell surface molecules first identified in NK cells (2B4 and NCRp1-a[31]); signal transduction molecules (DAP12 and FcεRγ) and transcription factors (Id2 and Ets-1) essential for NK cell differentiation[32,33]; and diverse molecules that are shared among multiple cell types of the innate immune system (CCL5, CCR5, XDH and Pglyrp)[31,34,35]. The 'NK-related' transcripts represent 6 of the 30 most-induced genes, whereas the entire 'NK-related' component of the Mu74Av2 chip includes only 29 of its 12,488 elements (identified by annotation and literature search; $P < 10^{-10}$, chi-squared test). We then extracted the data for all of the NK cell–related genes on the chip (**Fig. 5b**, sorted by AA/AB ratio). The induced genes encoded mainly NK 'stimulatory' molecules involved in either NK cell differentiation or active natural killing, whereas those genes specifying NK 'inhibitory' molecules were for the most part unaltered or not expressed at all (**Fig. 5b**). Thus, a strong agonist signal induces thymocytes to activate genes involved in innate responses.

a

O	AB	AA	AA/AB (RMA)	AA/AB (MAS)	*P* value (-log10)	Gene product	AffyID
516.8	343.9	1562.5	4.54	5.13	3.38	Ccl5	98406_at
35.4	37.0	165.2	4.46	8.81	2.13	Car2	92642_at
29.3	21.3	91.9	4.31	8.73	4.05	Cd244	95380_at
181.5	80.4	335.6	4.18	7.44	1.36	Idb2	93013_at
258.8	242.6	947.8	3.91	5.08	1.50	EST	160255_at
349.4	172.1	625.8	3.64	3.62	1.74	Klrd1	93677_at
34.4	47.8	171.7	3.59	5.82	1.45	Kdt1	102644_at
55.2	59.5	179.5	3.02	3.59	1.27	Cd9	95661_at
84.0	91.1	272.9	3.00	3.2	2.25	EST	104056_at
141.6	138.3	404.7	2.93	5.61	1.67	Serpina3k	102860_at
102.7	56.7	164.1	2.90	3.12	1.11	Cxcr4	93043_at
23.7	27.0	77.0	2.85	2.18	1.24	Tnfsf11	93416_at
76.4	91.9	251.3	2.74	3.59	1.11	EST	102914_s_at
416.6	308.9	824.1	2.67	5.82	3.52	Anxa2	100569_at
18.4	25.4	67.7	2.66	4.41	1.09	Kit	99956_at
22.1	30.5	80.2	2.63	2.9	0.60	Blk	95893_at
25.3	71.9	189.1	2.63	3.35	0.80	Ahr	160495_at
20.7	20.6	51.9	2.52	7.16	1.93	Klrb1a	94772_at
25.8	18.3	44.7	2.44	3.47	0.79	Ccr5	161968_f_at
49.5	58.9	142.8	2.43	2.59	1.55	EST	102920_at
36.6	40.5	95.3	2.36	2.84	1.49	Tyrobp	100397_at
96.8	96.9	226.6	2.34	2.98	1.47	Psen2	99930_s_at
40.4	44.4	99.1	2.23	3.54	4.16	Plscr1	102839_at
72.3	76.9	170.4	2.22	2.7	1.12	Smpdl3a	94872_at
60.8	75.1	165.2	2.20	2.48	2.44	EST	101001_at
28.1	30.6	67.4	2.20	3.15	1.34	Wbscr5	103690_at
38.2	31.2	66.8	2.15	3.65	0.46	EST	96605_at
81.6	59.8	127.5	2.13	3.1	1.09	Hmgb1	93095_at
82.5	72.7	150.0	2.06	2.55	0.78	Cab39	93976_at
36.9	40.5	82.9	2.05	3.49	1.06	EST	103560_at
182.5	128.5	259.9	2.02	5.3	0.60	EST	103889_at
19.7	20.3	40.9	2.02	3.09	1.08	Myo1e	92277_at
25.4	25.9	51.6	1.99	3.35	0.42	EST	92282_at
299.6	370.7	735.4	1.98	2.61	0.69	Vps54	102670_at
51.3	57.8	114.4	1.98	2.11	4.21	Pscd3	103433_at
114.5	115.8	226.6	1.96	3.28	0.88	EST	96191_at
26.8	35.8	69.7	1.94	3.11	0.86	Wsb1	98946_at
56.9	47.7	92.2	1.93	3.6	0.65	Ube2e1	92660_f_at
55.3	44.3	84.9	1.91	2.49	1.13	Gna13	104316_at
125.9	132.4	250.4	1.89	4.6	0.68	Cxcr3	94173_at
38.4	51.7	97.1	1.88	2.43	0.87	EST	104177_at
10.2	10.4	19.3	1.86	3.25	0.88	EST	160906_i_at
23.6	32.2	58.7	1.82	2.72	1.53	Cyfip1	102752_at
21.8	22.1	40.3	1.82	2.36	1.96	EST	102645_at
47.3	46.8	84.6	1.81	3.56	1.20	H1f0	95419_at
18.5	26.9	47.2	1.75	2.17	0.63	Ifit2	103639_at
26.1	23.3	40.3	1.73	3.38	1.63	Gzmc	102733_at
145.0	123.2	210.1	1.71	3.23	0.78	Nsmaf	160826_at
31.1	37.2	63.3	1.70	3.86	1.08	EST	95559_at
77.2	97.3	165.1	1.70	2.22	1.01	Igf2r	95117_at
103.7	121.7	204.6	1.68	2.14	1.02	Egr2	102661_at
612.2	655.7	1099.5	1.68	3.05	0.17	Ly6c	93077_s_at
49.5	70.2	117.3	1.67	3.13	0.63	EST	104586_at
132.5	171.1	279.0	1.63	2.1	0.68	Ifi205	94224_s_at
52.2	54.6	88.8	1.63	2.99	0.43	EST	97967_at
46.2	41.8	67.4	1.61	1.91	0.87	Ets1	94332_at
75.8	116.7	187.9	1.61	2.37	0.61	Qk	95096_at
19.1	22.8	36.4	1.60	3	0.74	Nr4a2	92248_at
85.4	98.6	157.4	1.60	3.82	0.94	EST	93465_at
13.5	12.7	20.3	1.59	2.62	0.02	Ell2	103891_i_at
20.7	20.2	31.7	1.57	4.5	1.82	Xdh	97950_at
151.7	159.9	249.8	1.56	2.23	1.21	EST	94759_at
62.6	104.4	162.9	1.56	5.35	0.65	Wbscr5	161899_f_at
22.3	23.1	35.4	1.53	2.64	0.93	Rbl2	95617_at
19.1	21.0	32.0	1.53	3.72	0.94	Pglyrp	162475_f_at
61.9	51.6	78.6	1.52	3.94	0.61	Capg	160106_at
55.7	68.6	102.2	1.49	2.32	0.84	Gbp3	103202_at
21.8	23.2	34.4	1.49	2.92	1.86	Tnfsf6	97113_at
22.1	20.5	30.4	1.48	3.7	0.64	Numb	99955_at
56.8	61.5	90.6	1.47	2.15	0.41	Pglyrp	104099_at
76.5	79.7	116.4	1.46	4.33	1.31	Klrb1c	93380_at

b

O	AB	AA	AA/AB (RMA)	AA/AB (MAS)	*P*-value (-log10)	Gene product	AffyID
29.3	21.3	91.9	4.31	8.73	4.05	Cd244	95380_at
181.5	80.4	335.6	4.18	7.44	1.36	Idb2	93013_at
349.4	172.1	625.8	3.64	3.62	1.74	Klrd1	93677_at
18.4	25.4	67.7	2.66	4.41	1.09	Kit	99956_at
20.7	20.6	51.9	2.52	7.16	1.93	Klrb1a	94772_at
36.6	40.5	95.3	2.36	2.84	1.49	Tyrobp	100397_at
182.7	202.8	412.6	2.04	2.96	1.25	Cd160	102272_at
46.2	41.8	67.4	1.61	1.91	0.87	Ets1	94332_at
76.5	79.7	116.4	1.46	4.33	1.31	Klrb1c	93380_at
25.5	24.9	33.2	1.34	2.25	0.59	Il18r1	101144_at
19.1	21.6	27.9	1.29	6.71	1.00	Fcer1g	162181_f_at
45.4	41.4	51.3	1.24	2.12	0.85	Il15ra	161023_at
45.4	51.0	63.0	1.24	2.05	0.79	Il12rb1	98240_at
16.6	17.3	21.2	1.23	1.37	0.60	Klra5	100673_f_at
98.6	104.9	119.3	1.14	1.66	0.18	Klrb1b	94744_at
43.9	49.4	55.5	1.12	1.66	0.68	Lag3	98392_at
22.2	21.3	22.7	1.07	1	0.59	Klra9	94779_f_at
19.2	20.6	21.8	1.06	2.67	0.59	Klrk1	93679_at
23.0	24.1	25.2	1.05	2.66	0.25	Klra6	100674_f_at
16.2	16.4	17.1	1.04	0.52	0.07	Klra7	97762_f_at
11.8	11.9	12.3	1.04	1.86	0.16	Klra4	94776_f_at
14.0	14.0	14.4	1.03	1.3	0.03	Klra3	93894_f_at
14.1	11.8	12.0	1.02	1	0.17	Klra2	98801_at
97.5	96.1	93.2	0.97	2.19	0.03	Elf4	98289_at
19.9	19.9	19.2	0.96	0.81	0.04	Klra7	97761_f_at
13.3	13.5	13.0	0.96	1.25	0.68	Klra8	100326_f_at
14.0	13.8	13.0	0.95	1.44	0.08	Klra3	93893_f_at
14.8	11.7	10.9	0.93	0.87	0.23	Ncr1	97781_at
10.2	10.9	10.1	0.93	1.2	0.34	Klra1	95908_at
12.9	11.3	10.4	0.92	0.9	0.21	Klra9	100387_f_at
26.6	28.3	22.6	0.80	0.54	0.85	Klrc1	99370_at

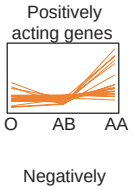

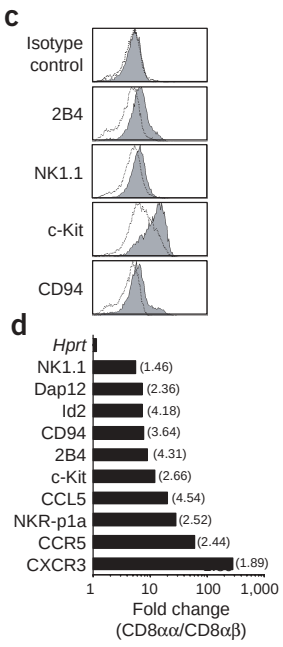

Figure 5 Integrated set of genes involved in innate or NK function induced by agonist in TCRαβ T cells. (**a**) Genes over-represented in AA relative to AB and O sets are ordered by AA/AB ratio. Data include the 'distilled' expression value (RMA algorithm, which produces individual values less contaminated by noise from 'mismatched probe' signals), the AA/AB ratio, the uncorrected *P* value of the AA/AB comparison (Welch's *t*-test), the gene product identity and the Affymetrix ID (AffyID). As RMA normalization tends to underestimate 'fold changes', the AA/AB ratio from MAS processing is included. Orange, involved in innate or NK cell differentiation and function. (**b**) The induction of NK-related genes in CD8αα cells involves only stimulatory (orange), not inhibitory (blue), genes. This annotation list of all NK-related genes represented on the Mu74Av2 chip (including surface receptors, transcription factors, or transduction molecules) was prepared from data on the Affymetrix or TIGR websites. Data are presented as described in **a**, with correlated expression plots (as described in **Fig. 4c**) shown for stimulatory or inhibitory genes (right). (**c**,**d**) Verification of the gene expression data. Expression of several upregulated genes in CD8αα (shaded) or CD8αβ (dotted lines) cells was verified by flow cytometry (**c**) or by quantitative real-time PCR (**d**; gene products, left margin) with CD8αβ or CD8αα thymocytes sorted from female or young male HY-TCR *Rag2*$^{-/-}$ ($H2^{b}$) mice. Values are expressed relative to CD8αβ; Hypoxanthine guanine phosphoribosyl transferase transcripts (*Hprt*) were quantified as an internal standard. Values in parentheses (**d**) indicate 'fold changes' in the microarray data.

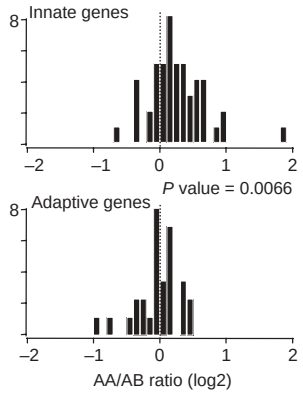

b Innate genes overexpressed in AA

AB	AA	AA/AB (RMA)	B2-B Sp.B6	CD4-T Sp.B6	CD8-T naive	DC LN	NK Sp.NOD	NK Sp.B6g7	Gene product	AffyID
206.3	762.6	3.70	63.8	175.9	83.4	2163.1	217.2	573.6	Ccl5	98406_at
65.3	130.4	2.00	57.9	136.9	78.4	185.1	215.1	183.7	Cd9	95661_at
55.2	103.8	1.88	78.3	59.6	66.8	191.9	193.5	413.0	Car2	92642_at
112.4	196.1	1.74	47.6	263.5	150.0	966.3	213.2	477.7	Idb2	93013_at
49.1	79.2	1.61	33.5	33.7	39.5	82.5	74.1	111.5	Cd244	95380_at
89.1	143.6	1.61	185.1	175.7	160.7	583.4	360.8	375.0	Sat1	96657_at
82.1	131.2	1.60	88.5	69.2	90.8	440.7	326.8	501.1	Lst1	103571_at
45.9	71.0	1.54	32.0	44.4	37.1	107.6	192.3	347.8	Ccr5	161968_f_at
52.0	78.8	1.51	65.6	43.0	57.5	336.5	468.0	960.2	Tyrobp	100397_at
281.8	420.1	1.49	76.7	119.9	116.3	586.3	515.3	509.8	Anxa2	100569_at
54.8	80.9	1.48	103.0	87.9	58.3	601.6	154.8	162.8	Rgs2	97844_at
59.0	86.2	1.46	50.5	55.8	51.9	149.4	152.8	104.1	Plscr1	102839_at
61.0	85.1	1.39	58.0	52.4	49.3	126.2	139.3	136.3	Litaf	93753_at
230.3	311.6	1.35	372.6	461.4	259.2	739.5	852.6	1008.2	Itm2b	101123_at
340.3	459.0	1.35	135.0	119.8	134.7	1051.8	275.2	365.8	Atpi	93984_at
78.7	103.4	1.31	108.1	91.3	72.4	374.1	213.0	119.1	Ev12a	98025_at

Adaptive genes overexpressed in AB

AB	AA	AA/AB (RMA)	B2-B Sp.B6	CD4-T Sp.B6	CD8-T naive	DC LN	NK Sp.NOD	NK Sp.B6g7	Gene product	AffyID
241.5	122.5	0.51	207.8	423.2	423.2	103.1	65.2	76.2	Satb1	99665_at
247.6	146.1	0.59	307.0	810.6	367.8	133.8	229.4	214.9	EST	96791_at
193.5	143.4	0.74	314.5	430.3	176.6	94.9	164.7	124.2	Klf3	100011_at

Figure 6 Innate-like character of the transcriptional patterns in CD8αα cells. A broad population analysis was done with Mu74Av2 data sets generated from cells typical of the innate (lymph node DCs and splenic NK cells from NOD or B6g7 background) or adaptive immune systems (splenic B2-B and CD4$^+$, lymph node CD8$^+$ T cells). These data sets were normalized and 'cross-compared', defining innate- and adaptive-like genes as those that showed consistently higher expression in every pairwise comparison between innate or adaptive cells (primary 'fold change' > 2). (**a**) Expression ratio in CD8αα versus CD8αβ. The distribution of 'innate genes' over-represented in CD8αα cells is skewed compared with that of 'adaptative genes' over-represented in CD8αβ cells. Vertical axes, numbers of genes. (**b**) Lists and expression values of the genes presented in **a**.

We did several experiments to confirm the microarray observations. Flow cytometric analyses confirmed the presence of 2B4, NK1.1, c-Kit and CD94 at the surface of CD8 SP cells from agonist-stimulated RTOC (**Fig. 5c**), although in much lower amounts than in mature NK or IELs stained with the same reagents (data not shown). We also verified that the innate profile exists *in vivo* by sorting CD8αα SP cells from neonatal HY male thymi (as in **Fig. 2b**) and analyzing their RNA by real-time quantitative PCR (**Fig. 5d**). All 11 transcripts tested showed a notable increase relative to that of conventional CD8αβ SP cells from thymi of adult female mice. The 'fold induction' between CD8αα and CD8αβ reproduced the chip results, albeit with far greater 'fold changes' (ranging from 8- to 300-fold; this higher differential was expected, as DNA chips are known to substantially under-represent 'fold changes').

To confirm that the apparent innate characteristics of the CD8αα cell transcriptional program, we did a multipopulation computational analysis. We grouped microarray data sets from several experiments done in similar conditions in the laboratory, defining typical adaptive (B2-B, CD4$^+$ and CD8$^+$ lymphocytes) and innate (dendritic and NK cells) cell groups. We classified innate-like genes and adaptive-like genes as those showing consistent differential expression in every pairwise comparison between members of innate or adaptive groups (that is, those overexpressed in both DC and NK cells relative to all lymphocytes); 50 and 29 genes, respectively, matched these definitions. We then compared their expression in CD8αα and CD8αβ cells (**Fig. 6**). Although the differences were not 'all-or-none', there was a very distinct skewing of the innate-like genes, which were over-represented in the CD8αα cells ($P < 0.02$, two-tailed paired *t*-test), whereas adaptive-like genes were over-represented in CD8αβ cells ($P < 0.007$, aggregate unpaired *t*-test). With the exception of the gene encoding 2B4, none of the innate-like genes would be considered typical NK genes (**Fig. 6b**, filtered on AA/BB 'fold changes' > 1.3). The presence of Id2 in this list is 'comforting', given its function in both DC and NK cell but not T cell development[32,36]. These results further support the contention that the downregulation of *Cd8b* is not an isolated event to allow escape from negative selection but represents true lineage and transcriptional pattern shifts.

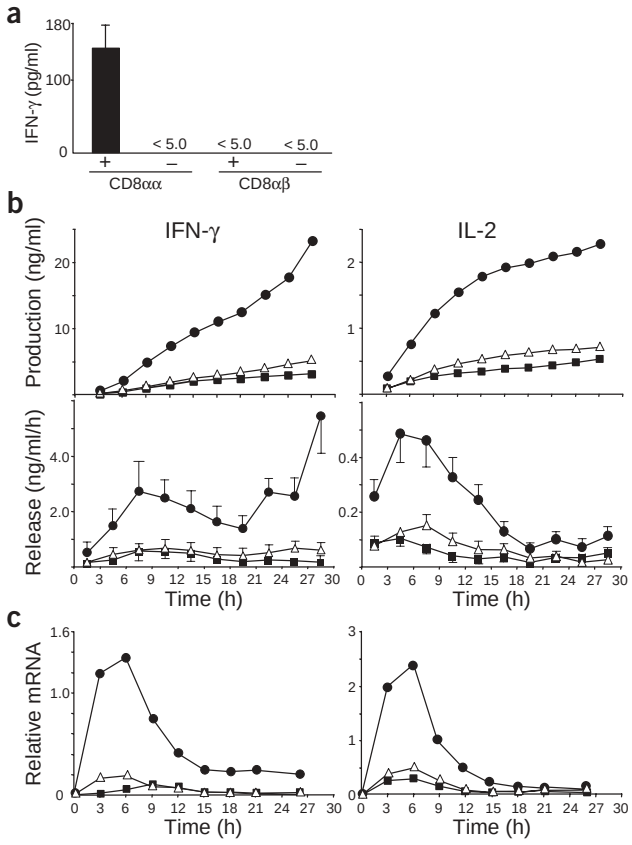

Figure 7 The density of TCR triggering in developing thymocytes engages an innate or an adaptive differentiation program. (**a**) IFN-γ production elicited by culture of sorted CD8αα or CD8αβ thymocytes (from young HY-transgenic male or female mice, respectively), stimulated with plate-bound anti-NK1.1. (**b**) Thymocytes (sources as described in **a**) were stimulated with plate-bound anti-CD3ε, and then IL-2 or IFN-γ production was measured at different times after stimulation. Top, total amount of cytokines produced; bottom, hourly release of the cytokines measured every 3 h. Results are representative of three or more experiments. ●, HY CD8αα; ■, HYCD8αβ; △, B6 CD8αβ. (**c**) RNA was prepared from cultures similar to those in **b**, and IFN-γ or IL-2 mRNA was quantified by real-time PCR, relative to hypoxanthine guanine phosphoribosyl transferase transcripts used as a standard.

Innate-like responses of CD8αα thymocytes

These observations suggested that CD8αα thymocytes are endowed with properties to equip them to participate in the innate immune response. To test this, we first examined the functional competence of NK1.1 molecules on the surface of CD8αα thymocytes. We sorted CD8αα or CD8αβ thymocytes from male or female HY TCR–transgenic mice as mature $TCR^{hi}HSA^{lo}$ cells to exclude preselected immature thymocytes. Crosslinking of NK1.1 induced secretion of IFN-γ from CD8αα but not from CD8αβ thymocytes, indicating that the surface NK1.1 molecule whose expression was detected in the microarray analysis was indeed functional (**Fig. 7a**).

Innate immune responses are characterized by an immediate effector function[37], whereas adaptive immunity normally requires several days of priming before full effector activity and cytokine production are manifest. Thus, we obtained HSA^{lo} CD8αβ or CD8αα thymocytes derived from adult female or young male HY TCR–transgenic mice, or from thymi of control B6 mice, simulated these cells with anti-CD3 and examined the kinetics of secretion of IFN-γ and interleukin 2 (IL-2). CD8αα thymocytes rapidly secreted IFN-γ and IL-2, with a first secretion peak around 6–9 h, followed by a secondary surge after 24 h for IFN-γ secretion (**Fig. 7b**). In contrast, IFN-γ and IL-2 production by CD8αβ thymocytes was slow and progressive.

We then sought to determine whether accelerated cytokine secretion by CD8αα cells stimulated with anti-CD3 was due to release of intracellular stores or to fast transcriptional induction. We prepared RNA from cultures of sorted HY CD8αβ or CD8αα thymocytes at different times after anti-CD3 stimulation to measure IFN-γ and IL-2 mRNA by real-time quantitative PCR (**Fig. 7c**). CD8αα thymocytes showed a very rapid accumulation of IFN-γ and IL-2 message, peaking at 3–6 h after stimulation. Thus, the cytokine genes in agonist-selected CD8αα thymocytes are poised for immediate transcriptional response to TCR triggering. In contrast, CD8αβ thymocytes show minimal responsiveness of cytokine genes.

DISCUSSION

Potentially autoreactive lymphocytes with self-reactive receptors arise inevitably from the combinatorial rearrangement of somatically variable TCR and B cell receptor genes, but this is the 'price' that the adaptive immune system must 'pay' for adaptability. The dogma has been that such cells must be destroyed or inactivated in the thymus before they have the opportunity to wreak havoc in the periphery[12,13]. However, observations made over the last 15 years have been inconsistent with this simple view. The results described here provide strong support for the idea that recognition of agonist peptide by immature DP thymocytes can modify primary transcription programs.

We applied microarray testing of gene expression, a potentially powerful approach for 'dissecting' elaborate cell differentiation programs, to analyze thymocyte positive selection, using an RTOC system that circumvents several theoretical difficulties. Using DP cells from a strictly nonselecting background and inducing their differentiation with known exogenous peptide provides very synchronous and homogeneous populations, more suitable for microarray analysis than those provided by the heterogeneous maturation states and selecting peptides of *in vivo* populations.

Self peptide at doses equivalent to those that optimally stimulate splenic T cells elicits an alternate differentiation program: in addition to *Cd4*, *Cd8b* was shut off, and a set of genes typical of innate or NK cell differentiation and activity was turned on. At first glance these findings may seem discordant with the prevailing view of the HY TCR–transgenic system as a paradigm for clonal deletion of thymocytes bearing self-reactive TCRs; in fact, they are consistent with many previous observations. Many HY TCR–bearing T cells can escape elimination in male thymi[19,27,38–40]. Such escapees have been attributed either to a dampened reactivity mediated by coreceptor downmodulation or to inappropriate expression of the transgene-encoded HY TCR by cells of the γδ lineage[24,39]. It has also been reported that gut IELs are abundant in HY TCR-transgenic male mice[19,20]. Our data show that the nature of these survivors varies over time: in young mice, they are CD8αα cells similar to those elicited by RTOC, whereas in adults they show dull expression of the CD8αβ coreceptor and are most likely those ascribed to misrouting into the γδ lineage[39]. CD8αα thymocytes do derive from DP cells through a positive selection process, with the usual kinetics and acquisition of maturation markers. Therefore, they do not result from an early branching off from DN precursors and do not belong to the γδ lineage, as confirmed by the lack of induction of TCRγδ expression in the microarray data. Furthermore, this type of lineage commitment is independent of the MHC restriction element, an observation probably related to the increase in MHC class II–restricted CD8 SP cells noted in agonist-stimulated FTOC[29].

Downmodulation of CD8β in FTOC systems supplemented with agonist to unselected DP cells has also been reported, and this was interpreted as a 'tuning' of signaling intensity that allowed maturing T cells to survive or was attributed to a deviation along a γδ-like pathway[22–24]. Our analyses indicate that a broader programmatic change takes place, rather than a simple 'dodge' of negative selection.

It is this overall pattern of gene expression changes that gives the most fascinating glimpse into the possible function of the differentiative program generated in this way. Two elements seem key. The shut-off of CD8β gene expression, in a single molecular switch, eliminates the CD8αβ coreceptor required for effective signaling 'downstream' of classical TCR–MHC class I molecule engagements and brings out the CD8αα coreceptor, a TCR-independent ligand for the nonclassical MHC class I molecule TL[41]. Moreover, a broader programmatic change activates a panel of genes typical of the innate immune system, ranging from cell surface receptors to signaling molecules or transcription factors, several of which are essential to the differentiation and function of innate immune system cells: NK receptors (NCRs), DAP12, FcεRγ, c-Kit and so on. Most provocative is the strong induction of Id2, a member of the 'inhibitor of DNA binding' family and a key factor for NK cell and DC development[32,36]. The Id2 overexpression in CD8αα cells is accompanied by a downregulation of E2A, which has an effect exactly the opposite to that of Id2 on the NK cell–T cell balance[42]. Id2 and E2A might be the direct downstream targets of strong TCR engagement and might control the other changes.

Does this induction of typical innate response genes have functional consequences? It is notable that the coordinated induction of a subset of NK cell–specific genes seems to favor the stimulatory receptors and other facilitators of NK cell function, rather than inhibitors. However, some of the overexpressed genes, such as the gene encoding 2B4, can have opposite effects depending on their binding partners or splicing forms. We have shown that some of these molecules are indeed functional, but also that CD8αα cells have adopted the 'hair-trigger' reactivity characteristic of innate response cells such as mast or NK cells. This effect is manifest at the transcriptional level, and the *Infg* locus may adopt in CD8αα cells a chromatin configuration different from that formed in conventional naive T cells.

CD8αα SP cells are endowed with a complex set of surface receptors: a TCR-coreceptor complex with high affinity for an epithelial cell ligand, but one that is 'defused' and unable to signal fully, a set of NCRs and the CD8αα molecule. In this context, the self-reactive TCR might provide survival signals, as for conventional CD8αβ T

cells, consistent with the observation of short persistence of IELs without their eliciting stimulus[43]. Alternatively, stimulatory NCRs may act in synergy with self-recognizing TCRs and with CD8αα to sense quantitative variations in arrays of surface ligands on target cells, modified by infection and/or stress, with the TCRs sensing variation of MHC molecules secondary to inflammation[44] and the NCRs responding to increases in MHC class I–like molecules (RAE-1 or H60, and MICA or MICB[45]). The outcome of this stimulation might then be defensive or regulatory.

There is an interesting parallel between the selection of CD8αα cells and the terminal differentiation of mature CD8$^+$ T cells into memory phenotypes, which display NCRs and acquire rapid response characteristics[46]. It has been proposed that NCRs on CD8 memory cells serve to dampen secondary responses, but whether the broader innate-like characteristics of CD8αα cells also extend to memory populations remains to be determined.

Although we do not have direct evidence that the CD8αα SP thymocytes we described using RTOC are thymic IEL precursors[21], many elements argue in favor of this contention. The CD8αα phenotype, expression of the FcεRγ signal transduction molecule and NK cell–related transcripts were also detected by SAGE analysis of IELs[47]. Most relevant here, the emergence of IELs from the thymus is driven by agonist recognition[21,43]. The observation extended to several TCRs and was also independent of MHC restriction, and it was proposed that this selection pathway allows the immune system to preserve TCRs with high affinity for self, partially inactivated by the absence of CD8β. Our data suggest that the IEL pathway may branch off at the DP stage, meaning that DP thymocytes have several options for differentiation beyond the conventional CD4$^+$ and CD8$^+$ lineages. Our data also suggest that IELs may be generated preferentially in the post-natal period in normal mice, in the very first weeks of age, with a shift away from the CD8αα phenotype in adult mice.

CD8αα T cells elicited by expression of self antigen in the thymus seem to join B-1 B cells and CD4$^+$ NK T cells[37] to constitute a class of unconventional lymphocytes with features in common: expression of molecules characteristic of NK cells, recognition of self molecules and anatomical locations other than the principal lymphoid organs. Lymphocytes of the innate immune system often express germline-encoded and inherently self-reactive antigen receptors, and there has been some debate over whether their specialized phenotype predicates their self-reactivity or vice versa. Our results demonstrate a direct link, indicating that self-recognition is a primary trigger for 'donning' such characteristics.

In conclusion, the recognition of self antigens by members of the adaptive immune system does not necessarily lead to their elimination, but can modify primary transcriptional programs. The high-affinity receptor for self is reused, perhaps to monitor perturbations of self by collaborating with NCRs. This might have been the ancestral function of the TCR-MHC couple before TCR gene rearrangements brought variability and therefore adaptive potential.

METHODS

Mice. C57BL/6 mice were obtained from The Jackson Laboratory; HY-TCR *Rag2*$^{-/-}$ mice on nonselecting B10.D2 and selecting C57BL/10 backgrounds were obtained from Taconic Farms. The 5c.c7-TCR *Rag2*$^{-/-}$ mice on the nonselecting H-2^b background were provided by B.J. Fowlkes (National Institutes of Health, Bethesda, Maryland), and OT1-TCR *Rag2*$^{-/-}$ mice deficient in transporter associated with antigen processing were provided by J. Kirchner and M. Bevan (University of Washington, Seattle, Washington). All mice were bred and maintained in sterile barrier conditions at the Harvard Center for Animal Resources and Comparative Medicine (protocol 2954) in accordance with National Institutes of Health guidelines.

Thymic RTOC. The culture procedure mainly followed a published procedure[16]. Fetal thymic lobes at embryonic day 15 from C57BL/6 or invariant chain–null mice were cultured for 5 d in 1.35 mM deoxyguanosine (Sigma), and the gender of each embryo was determined by PCR genotyping for the sex-determining region of chromosome Y (*Sry*) with primers 5′-GTTCAGC-CCTACAGCCACAT-3′ and 5′-CACTTTCGCCCTCCGATGAG-3′. The lobes were dissociated with 0.05% trypsin plus 1 mM EDTA for preparation of TSCs. CD4$^+$CD8$^+$ thymocytes (DP) from 2-week-old mice were purified to >99% purity by magnetic sorting on either anti-CD4 or anti-CD8 beads (MACS; Miltenyi Biotec). Reaggregates were formed by mixing of TSCs and DP thymocytes at a cell ratio of 1:1 (5×10^5 cells each) and pelleting by centrifugation (855*g* for 2 min), and the cell slurry (4 μl) was carefully applied on the upper membrane of Transwell (Coaster) as a standing drop. The reaggregates were cultured for 4–8 d at 37 °C at 5% CO_2 in DMEM with 10% FCS, 10 mM HEPES, 50 μM β-mercaptoethanol, 2 mM L-glutamine and 0.1 mM nonessential amino acids, plus penicillin and streptomycin, either supplemented with peptide (Smcy, KCSRNRQYL; ovalbumin peptide, SIINFEKL; moth cytochrome c peptide, ANERADLIAYLKQATK; all high-performance liquid chromatography grade from Peptron) or not; medium and peptide were exchanged every day.

Flow cytometry. Cell surface molecules were stained with anti-CD4 (RM4-5), anti-CD8β (53-5.8) anti-TCRβ (H57-597), anti-$V_β$8 (F23.1), anti-HAS (M1/69), anti-CD244.2 (2B4), anti-CD94 (18d3), anti-NK1.1 (PK136; all from PharMingen); anti-CD8α (CT-CD8a), anti-K^b (CTKb; both from Caltag); anti-CD117 (2B8; eBioscience); or fluorescein isothiocyanate–conjugated peanut agglutinin (Sigma). Dead cells were excluded from analysis and sorting with 7-amino-actinomycin D (PharMingen) or Hoechst 33342 (Calbiochem) staining. Samples were analyzed on a Coulter XL cytometer with Expo32 software.

***In vitro* responses.** CD8 SP cells from RTOCs at day 8 were sorted (5×10^4 cells; MoFlo), were mixed with 5×10^5 stimulator splenocytes from B6 female mice plus 'graded' concentrations of Smcy peptide, and were cultured for 48 h and pulsed with [^{3}H]thymidine in the last 12 h before being collected and counted. Alternatively, stimulators were splenic DCs from male or female B6 mice. Whole splenocytes and DCs were irradiated with 2,000 rad before use. For thymocyte stimulations, HSA^{lo}TCR^{hi} CD8αβ thymocytes were sorted from B6 or female HY TCR *Rag2*$^{-/-}$ (H2^b) mice, and HSA^{lo}TCR^{hi} CD8αα thymocytes were sorted from young male HY TCR *Rag2*$^{-/-}$ (H2^b) mice. Thymocytes were stimulated with plate-bound anti-NK1.1 or anti-CD3 and supernatants were collected at 48 h for NK1.1 stimulation or every 3 h for CD3 stimulation.

Enzyme-linked immunosorbent assay. IFN-γ and IL-2 concentrations were measured by sandwich enzyme-linked immunosorbent assay with purified anti-mouse IFN-γ (R4-6A2) or anti-mouse IL-2 (JES6-1A12) as capturing antibody and biotinylated anti-mouse IFN-γ (XMG1.2) or anti-mouse IL-2 (JES6-5H4) as detection antibody (Pharmingen), respectively. Recombinant mouse IFN-γ or IL-2 (Pharmingen) was used as control reference.

Microarray analysis. RNA preparation and chip hybridizations were done as described[15]. HY CD8αα$^+$, HY CD8αβ$^+$ and OT1 CD8αβ$^+$ cells from RTOC at day 6 were purified by flow sorting. Total RNA from pooled cell populations (from approximately 3×10^4 cells) was immediately prepared with the High Pure RNA Isolation Kit (Roche) and was amplified for two rounds with the MessageAmp aRNA kit (Ambion), followed by biotin labeling with the BioArray High Yield RNA Transcription Labeling Kit (Enzo Diagnostics) and purification with the RNeasy Mini Kit (Qiagen). The resulting cRNA (four independent data sets for each of the three sample types) was hybridized to Affymetrix Mu74Av2 chips according to manufacturer's protocol. The initial 'reads' were processed through Affymetrix microarray Suite 5.0 software to obtain raw expression values. These were normalized and averaged (with outlier elimination), and an approximate measure of significance was calculated (Welch's approximation *t*-test) with custom 'scripts' (NORM and DISTILL; ref. 15) running on S-Plus software (Insightful). For analysis of significance, control data sets approximating the values and variances of the real data were generated by random reshuffling of the data (random draws within rows) or by simulated data sets

(random generation from gene-wise means and s.d.). Control genes (such as those expected to show differences depending on the origin of the input T cells, such as TCR V-region genes or chromosome X or chromosome Y genes; **Fig. 5a**) were verified and were removed for subsequent analyses. Informative gene sets were defined for noise reduction with thresholds on expression levels (>3, on a scale of 1–4,000) and on 'fold change' ratios (genes showing at least one 'fold change' greater than 2.5). Euclidian distances between populations were calculated (by SIMS script) for different 'fold change' thresholds as:

$$\sqrt{\Sigma(X_i - Y_i)^2}$$

from the real data and for random data sets; each *P* value was calculated as the probability of the observed distances relative to the mean and variance of the same distances in random data sets. Cluster analysis was done with the CORR script (data not shown), a 'supervised' method that groups genes based on correlation across all sample types (expression values normalized to the gene-wise expression mean, with a user-set correlation coefficient, set here at $r^2 = 0.95$).

Quantitative RT-PCR. RNA was isolated with Trizol (Invitrogen) followed by DNase treatment with DNA-*free* (Ambion). PCR was done with SYBR Green or Taqman Master Mix (Applied Biosystems). PCR and signal detection used a 7700 Sequence Detector (ABI Prism). Primers used for the reactions are available in **Supplementary Methods** online.

GEO accession number. Raw data sets, GSE 1112.

Note: Supplementary information is available on the Nature Immunology website.

ACKNOWLEDGMENTS

We thank L. Poirot, E. Venanzi and A. Goldrath for microarray data sets; Q.-M. Pham and V. Bruklich for help with the mice; G. Losyev for flow cytometry; R. Park for help with the data analysis; and the T cell group for discussions. Supported by the National Institutes of Health (1R01AI51530), by core services from the National Institute of Diabetes and Digestive and Kidney Diseases–funded Diabetes Endocrinology Research Center (Joslin Diabetes Center) and by the Japan Society for the Promotion of Science and the Uehara Memorial Foundation (T.Y.).

COMPETING INTERESTS STATEMENT

The authors declare that they have no competing financial interests.

Received 9 December 2003; accepted 15 March 2004
Published online at http://www.nature.com/natureimmunology/

1. Germain, R.N. T-cell development and the CD4-CD8 lineage decision. *Nat. Rev. Immunol.* **2**, 309–322 (2002).
2. Sebzda, E. *et al.* Positive and negative thymocyte selection induced by different concentrations of a single peptide. *Science* **263**, 1615–1618 (1994).
3. Ashton-Rickardt, P.G. *et al.* Evidence for a differential avidity model of T cell selection in the thymus. *Cell* **76**, 651–663 (1994).
4. Hogquist, K.A., Jameson, S.C. & Bevan, M.J. Strong agonist ligands for the T cell receptor do not mediate positive selection of functional $CD8^+$ T cells. *Immunity* **3**, 79–86 (1995).
5. Kawai, K. & Ohashi, P.S. Immunological function of a defined T-cell population tolerized to low-affinity self antigens. *Nature* **374**, 68–69 (1995).
6. Girao, C., Hu, Q., Sun, J. & Ashton-Rickardt, P.G. Limits to the differential avidity model of T cell selection in the thymus. *J. Immunol.* **159**, 4205–4211 (1997).
7. Wang, R., Nelson, A., Kimachi, K., Grey, H.M. & Farr, A.G. The role of peptides in thymic positive selection of class II major histocompatibility complex-restricted T cells. *Proc. Natl. Acad. Sci. USA* **95**, 3804–3809 (1998).
8. Kraj, P. *et al.* Positive selection of $CD4^+$ T cells is induced *in vivo* by agonist and inhibited by antagonist peptides. *J. Exp. Med.* **194**, 407–416 (2001).
9. Jordan, M.S. *et al.* Thymic selection of $CD4^+CD25^+$ regulatory T cells induced by an agonist self-peptide. *Nat. Immunol.* **2**, 283–284 (2001).
10. Apostolou, I., Sarukhan, A., Klein, L. & von Boehmer, H. Origin of regulatory T cells with known specificity for antigen. *Nat. Immunol.* **3**, 756–763 (2002).
11. Park, S.H. *et al.* The mouse CD1d-restricted repertoire is dominated by a few autoreactive T cell receptor families. *J. Exp. Med.* **193**, 893–904 (2001).
12. Burnet, F.M. A modification of Jerne's theory of antibody production using the concept of clonal selection. *C.A. Cancer J. Clin.* **26**, 119–121 (1976).
13. von Boehmer, H., Teh, H.S. & Kisielow, P. The thymus selects the useful, neglects the useless and destroys the harmful. *Immunol. Today* **10**, 57–61 (1989).
14. Schwartz, R.H. in *Fundamental Immunology* (ed. Paul, W.E.) 701–739 (Lippincott-Raven, Philadelphia, 1999).
15. Anderson, M.S. *et al.* Projection of an immunological self-shadow within the thymus by the aire protein. *Science* **298**, 139–1401 (2002).
16. Anderson, G., Jenkinson, E.J., Moore, N.C. & Owen, J.J. MHC class II-positive epithelium and mesenchyme cells are both required for T-cell development in the thymus. *Nature* **362**, 70–73 (1993).
17. Schulz, R.J., Parkes, A., Mizoguchi, E., Bhan, A.K. & Koyasu, S. Development of $CD4^-CD8^-$ αβ $TCR^+NK1.1^+$ T lymphocytes: thymic selection by self antigen. *J. Immunol.* **157**, 4379–4389 (1996).
18. Yasutomo, K., Doyle, C., Miele, L. & Germain, R.N. The duration of antigen receptor signalling determines $CD4^+$ versus $CD8^+$ T-cell lineage fate. *Nature* **404**, 506–510 (2000).
19. Rocha, B., von Boehmer, H. & Guy-Grand, D. Selection of intraepithelial lymphocytes with CD8α/α co-receptors by self-antigen in the murine gut. *Proc. Natl. Acad. Sci. USA* **89**, 5336–5340 (1992).
20. Cruz, D. *et al.* An opposite pattern of selection of a single T cell antigen receptor in the thymus and among intraepithelial lymphocytes. *J. Exp. Med.* **188**, 255–265 (1998).
21. Leishman, A.J. *et al.* Precursors of functional MHC class I- or class II-restricted $CD8\alpha\alpha^+$ T cells are positively selected in the thymus by agonist self-peptides. *Immunity* **16**, 355–364 (2002).
22. Chidgey, A. & Boyd, R. Agonist peptide modulates T cell selection thresholds through qualitative and quantitative shifts in CD8 co-receptor expression. *Int. Immunol.* **9**, 1527–1536 (1997).
23. Barnden, M.J., Heath, W.R. & Carbone, F.R. Down-modulation of CD8 β-chain in response to an altered peptide ligand enables developing thymocytes to escape negative selection. *Cell. Immunol.* **175**, 111–119 (1997).
24. Hogquist, K.A. & Bonnevier, J.L. Development of peptide-selected CD8 T cells in fetal thymic organ culture occurs via the conventional pathway. *J. Immunol.* **161**, 3896–3901 (1998).
25. Teh, H.S. *et al.* Early deletion and late positive selection of T cells expressing a male-specific receptor in T-cell receptor transgenic mice. *Dev. Immunol.* **1**, 1–10 (1990).
26. Teh, H.S., Kishi, H., Scott, B. & von Boehmer, H. Deletion of autospecific T cells in T cell receptor (TCR) transgenic mice spares cells with normal TCR levels and low levels of CD8 molecules. *J. Exp. Med.* **169**, 795–806 (1989).
27. Kisielow, P., Bluthmann, H., Staerz, U.D., Steinmetz, M. & von Boehmer, H. Tolerance in T-cell-receptor transgenic mice involves deletion of nonmature $CD4^+8^+$ thymocytes. *Nature* **333**, 742–746 (1988).
28. Berg, L.J., Frank, G.D. & Davis, M.M. The effects of MHC gene dosage and allelic variation on T cell receptor selection. *Cell* **60**, 1043–1053 (1990).
29. Kersh, G.J., Engle, D.L., Williams, C.B. & Allen, P.M. Ligand-specific selection of MHC class II-restricted thymocytes in fetal thymic organ culture. *J. Immunol.* **164**, 5675–5682 (2000).
30. Irizarry, R.A. *et al.* Summaries of Affymetrix GeneChip probe level data. *Nucleic Acids Res.* **31**, e15 (2003).
31. Moretta, A. *et al.* Activating receptors and coreceptors involved in human natural killer cell-mediated cytolysis. *Annu. Rev. Immunol.* **19**, 197–223 (2001).
32. Yokota, Y. *et al.* Development of peripheral lymphoid organs and natural killer cells depends on the helix-loop-helix inhibitor Id2. *Nature* **397**, 702–706 (1999).
33. Barton, K. *et al.* The Ets-1 transcription factor is required for the development of natural killer cells in mice. *Immunity* **9**, 555–563 (1998).
34. Luster, A.D. The role of chemokines in linking innate and adaptive immunity. *Curr. Opin. Immunol.* **14**, 129–135 (2002).
35. Vorbach, C., Harrison, R. & Capecchi, M.R. Xanthine oxidoreductase is central to the evolution and function of the innate immune system. *Trends Immunol.* **24**, 512–517 (2003).
36. Hacker, C. *et al.* Transcriptional profiling identifies Id2 function in dendritic cell development. *Nat. Immunol.* **4**, 380–386 (2003).
37. Bendelac, A., Bonneville, M. & Kearney, J.F. Autoreactivity by design: innate B and T lymphocytes. *Nat. Rev. Immunol.* **1**, 177–186 (2001).
38. Teh, H.S. *et al.* Thymic major histocompatibility complex antigens and the αβ T-cell receptor determine the CD4/CD8 phenotype of T cells. *Nature* **335**, 229–233 (1988).
39. Bruno, L., Fehling, H.J. & von Boehmer, H. The αβ T cell receptor can replace the γδ receptor in the development of γδ lineage cells. *Immunity* **5**, 343–352 (1996).
40. Buch, T., Rieux-Laucat, F., Forster, I. & Rajewsky, K. Failure of HY-specific thymocytes to escape negative selection by receptor editing. *Immunity* **16**, 707–718 (2002).
41. Gao, G.F., Rao, Z. & Bell, J.I. Molecular coordination of αβ T-cell receptors and coreceptors CD8 and CD4 in their recognition of peptide-MHC ligands. *Trends Immunol.* **23**, 408–413 (2002).
42. Bain, G. *et al.* E2A deficiency leads to abnormalities in αβ T-cell development and to rapid development of T-cell lymphomas. *Mol. Cell. Biol.* **17**, 4782–4791 (1997).
43. Capone, M. *et al.* Selective absence of $CD8^+$ $TCR\alpha\beta^+$ intestinal epithelial cells in transgenic mice expressing β_2-microglobulin-associated ligands exclusively on thymic cortical epithelium. *Eur. J. Immunol.* **33**, 1471–1477 (2003).
44. Gleimer, M. & Parham, P. Stress management: MHC class I and class I-like molecules as reporters of cellular stress. *Immunity* **19**, 469–477 (2003).
45. Natarajan, K., Dimasi, N., Wang, J., Mariuzza, R.A. & Margulies, D.H. Structure and function of natural killer cell receptors: multiple molecular solutions to self, nonself discrimination. *Annu. Rev. Immunol.* **20**, 853–885 (2002).
46. McMahon, C.W. & Raulet, D.H. Expression and function of NK cell receptors in $CD8^+$ T cells. *Curr. Opin. Immunol.* **13**, 465–470 (2001).
47. Shires, J., Theodoridis, E. & Hayday, A.C. Biological insights into $TCR\gamma\delta^+$ and $TCR\alpha\beta^+$ intraepithelial lymphocytes provided by serial analysis of gene expression (SAGE). *Immunity* **15**, 419–434 (2001).